PROCEEDINGS, 41st Workshop on Geothermal Reservoir Engineering
Stanford University, Stanford, California, February 22-24, 2016
SGP-TR-209

Numerical modeling of the Hágöngur Geothermal Reservoir in Central Iceland

Ximena Guardia Muguruza[1], Egill Júlíusson[2] and Ágúst Valfells[1]

[1]Reykjavík University, Menntavegur 1, 101 Reykjavik, Iceland

[2]Landsvirkjun, Háaleitisbraut 68, 103 Reykjavík, Iceland

ximena14 @ru.is

Keywords: Conceptual model, numerical model, natural state.

ABSTRACT

The Hágöngur geothermal area in Central Iceland is among the larger geothermal areas of the country. Surface exploration studies including geology and geothermal manifestations mapping, Transient Electromagnetic (TEM) resistivity surveys, Magnetotelluric (MT) soundings and geothermometry assessments have been conducted in the area, along with the drilling of one deep exploration well (HG-01) near the center of the resistivity anomaly. The present paper integrates all physical, geological and geochemical data available by developing conceptual and numerical models of the system, in order to provide insight into the reservoir's behavior for future utilization of the geothermal fluid.

Resistivity, lithology and stratigraphy models of the reservoir were created using the RockWorks16 software based on MT resistivity measurements, lithology data of the HG-01 borehole and geological and topographical information of the area. Two different versions of the conceptual model were built based on these data, plotting stratigraphy units, cap rock, faults, heat source, temperature gradients and flow pattern. Further numerical models were developed matching up stratigraphic elevation information, rock properties and downhole temperature and pressure values using the TOUGH2 simulator via the graphical user interface PetraSim. PetraSim was also employed to define and calibrate cell-specific data such as heat sources and initial conditions to create two versions of the natural state model of the reservoir.

1. INTRODUCTION

Several surface exploration studies were conducted in the Hágöngur geothermal area in order to estimate its potential. In 1995, geology features and geothermal manifestations were mapped, as there were plans to construct a hydro dam that would partially submerge the thermal site (Jonsson, Gudmundsson & Palsson, 2005). This research was followed by a resistivity survey using the Transient Electromagnetic (TEM) method in 1998 (Karlsdóttir & Vilhjálmsson, 2013), and in the next year, submersion of the thermal area finally took place (Jonsson, Gudmundsson & Palsson, 2005).

In 2003, the exploration well HG-01 was drilled up to a depth of 2360 meters near the center of the resistivity anomaly, confirming the existence of a high temperature geothermal system with temperatures up to 290-300°C in accordance with previous geothermometry assessments. Later on, in 2007 the initial TEM survey was extended, revealing a high temperature geothermal system of 40 km^2 of horizontal area at 800 meters depth (Karlsdóttir & Vilhjálmsson, 2013).

In 2011, a total of 16 Magnetotelluric (MT) soundings were performed in the same locations as the existing TEM soundings. A one dimension interpretation of the MT showed the presence of a deep seated low resistivity at depth, hence indicating the presence of a heat source in the geothermal system. Finally, during winter 2013, 14 MT soundings through ice were performed for the first time in Iceland on the Hágöngur Lake, followed by 6 more soundings in summer 2013. Results showed a deep seated low resistivity body as high as 1100 m.b.s.l. in the geothermal area (Karlsdóttir & Vilhjálmsson, 2013).

The present paper integrates all physical, geological, geochemical and downhole data available by developing different geologically consistent conceptual and numerical models of the system, in order to provide insight into the reservoir's behavior for future utilization of the geothermal fluid. The intention of building more than one version of the conceptual and natural state models is to account for uncertainty in the structure of the reservoir, as subsurface data is just available for one well in the middle of it and further subsurface geology is unknown.

2. METHODOLOGY

The elaboration of the paper involved an initial processing of all geological, geophysical, geochemical and downhole data available for the reservoir, through the usage of Geographic Information System (GIS) tools and 3D visualization software like RockWorks16, Google SketchUp and AutoCAD. In addition, stratigraphy models, resistivity data and estimated temperatures were used to create a few versions of the conceptual model of the reservoir in RockWorks16. Finally, there were developed two different versions of the natural state model of the reservoir using the TOUGH2 simulator and its interface PetraSim, as shown in Figure 1.

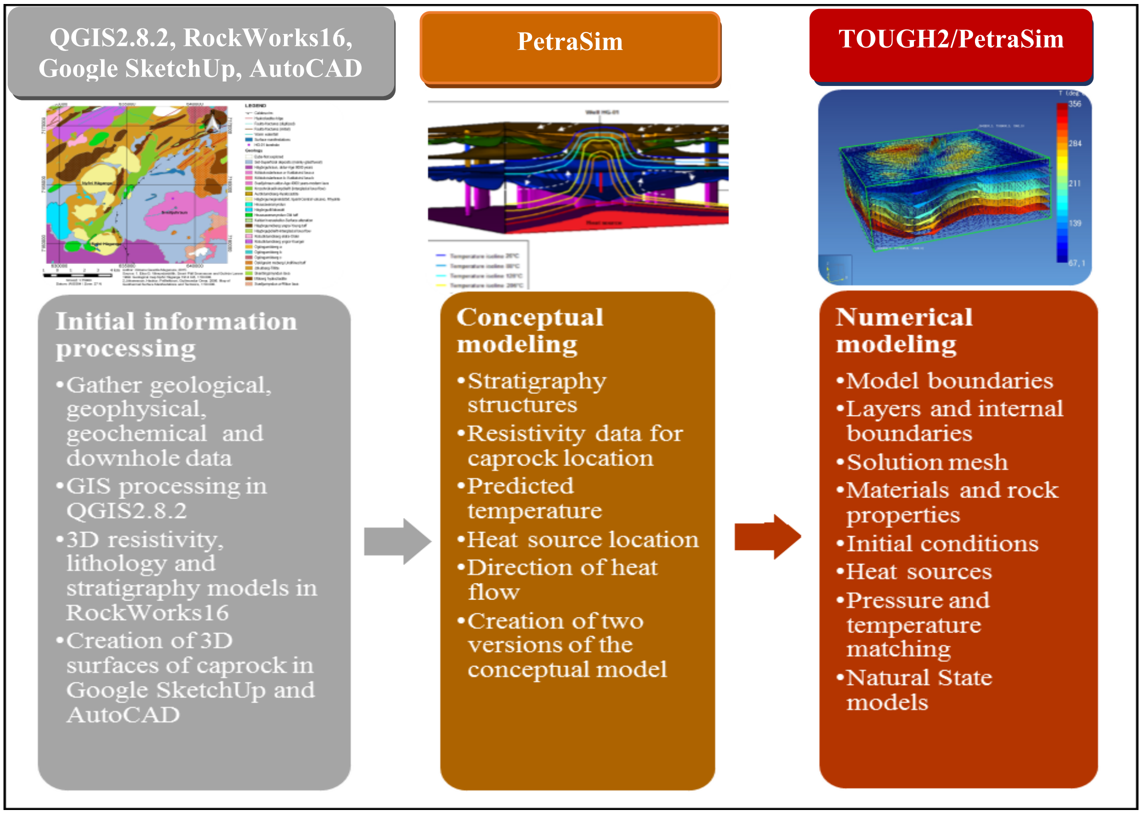

Figure 1: Methodology diagram.

Topography, geology, faulting, surface manifestation and resistivity data were gathered, digitized and overlapped using the QGIS2.8.2 Geographic Information System (GIS) software. Placement of point data values, as well as the extraction of specific information for each point was executed using the same software.

On the other hand, the RockWorks16 software was used to create resistivity, lithology and stratigraphy models of the reservoir, based on MT resistivity measurements, lithology data of the HG-01 borehole and geological and topographical information of the area extracted from QGIS2.8.2. Different stratigraphy profiles were created and exported as text files for the development of further natural state models.

Furthermore, Google SketchUp and AutoCAD software were employed for the creation of 3D triangular solid surfaces representing internal and external boundaries of the reservoir´s cap rock. These surfaces were exported as DXF files for their use in the subsequent numerical modeling.

Thereafter, more than one natural state model was built matching up stratigraphy elevation information, rock properties and temperature and pressure values, using the TOUGH2 simulator via the graphical user interface PetraSim. PetraSim was employed to establish boundaries, structure and properties of the reservoir in grid digitized models. Cell-specific data was defined and calibrated such as rock properties, heat sources and initial conditions to create two versions of the natural state model of the reservoir. Rock properties used for the development of the natural state models are presented in Table 1.

Table 1: Rock properties specified in the models (Sources 1, 2, 3, 4, 5, 6 and 7).

Name	Rock Density(kg/m^3)	Porosity (%)	X, Y, Z Permeability (mD)	Wet heat conductivity (W/m*°C)	Specific heat (J/kg*°C)
Tuff	2750[1]	27.8[1]	367 [1]	0.30 [2,5]	1100[3]
Rhyolite	2650[1]	11.6[1]	0.028 [1]	3.00 [2]	1060[2]
Basalt	2860[1]	7.1[1]	3.75 [1]	1.7 [4]	840 [5]
Dacite	1950 [6]	10[7]	1.01[7]	0.69 [2]	1170[2]

Note:
[1] Stefánsson, *et al.*., 1997, [2] Wohletz and Heiken, 1992, [3] Heiken, 2006, [4]Hjartarson, 2015, [5] Eppelbaum, Kutasov & Pilchin, 2014, [6] Ágústsdóttir, 2009 and Heiken, 2006, [7] Zou, 2013.

3. RESULTS

3.1 Initial Information Analysis

3.1.1 Geographical Information System Results

A map summarizing geology formations and location of faults, surface manifestations, caldera rim and other surface exploration features was developed for the Hágöngur area and is presented in Figure 2.

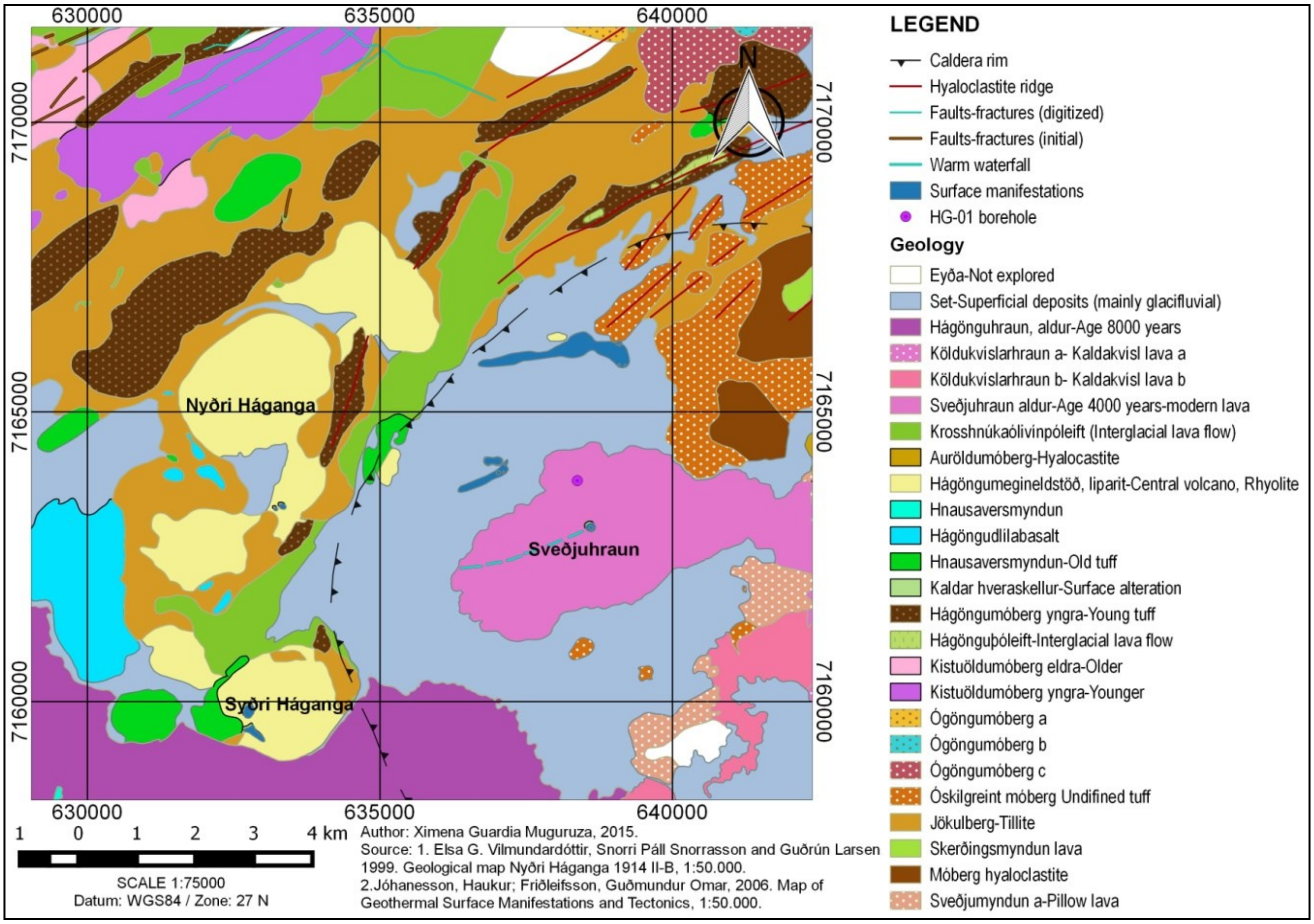

Figure 2: Surface exploration features of the Hágöngur area.

As seen in Figure 2, the reservoir is delimited by a caldera rim with faults and hyaloclastite ridges mostly on its North-East flank. Superficial geology in the eastern side of the caldera rim is composed mainly by glaciofluvial deposits, modern lava, tuff and hyaloclastite formations. On the other hand, the western side of the caldera rim is composed mainly by interglacial lava flows, rhyolite in the Nyðri and Syðry Háganga domes, surrounded by tillite and tuff ridges.

3.1.2 Resistivity model

A 3D solid model for resistivity created in RockWorks16 is shown in Figure 3. As seen in Figure 3 and in accordance to the 3D Inversion of MT Data developed for the reservoir, there is a low resistivity cap near surface, followed by a high resistivity core that denotes the area where the system has reached or/and exceeded temperature of 250°C (Karlsdóttir & Vilhjálmsson, 2013). Fractions of the low resistivity body are seen at depth, indicating the heat source of the geothermal system.

In spite of the proper resistivity structure along the models, not well defined low resistivity areas could be found, so conceptual and natural state models were developed on the basis of the resistivity results of the TEM survey of 2007 (Karlsdóttir *et al.*, 2007) and the 3D Inversion of MT Data (Karlsdóttir & Vilhjálmsson, 2013).

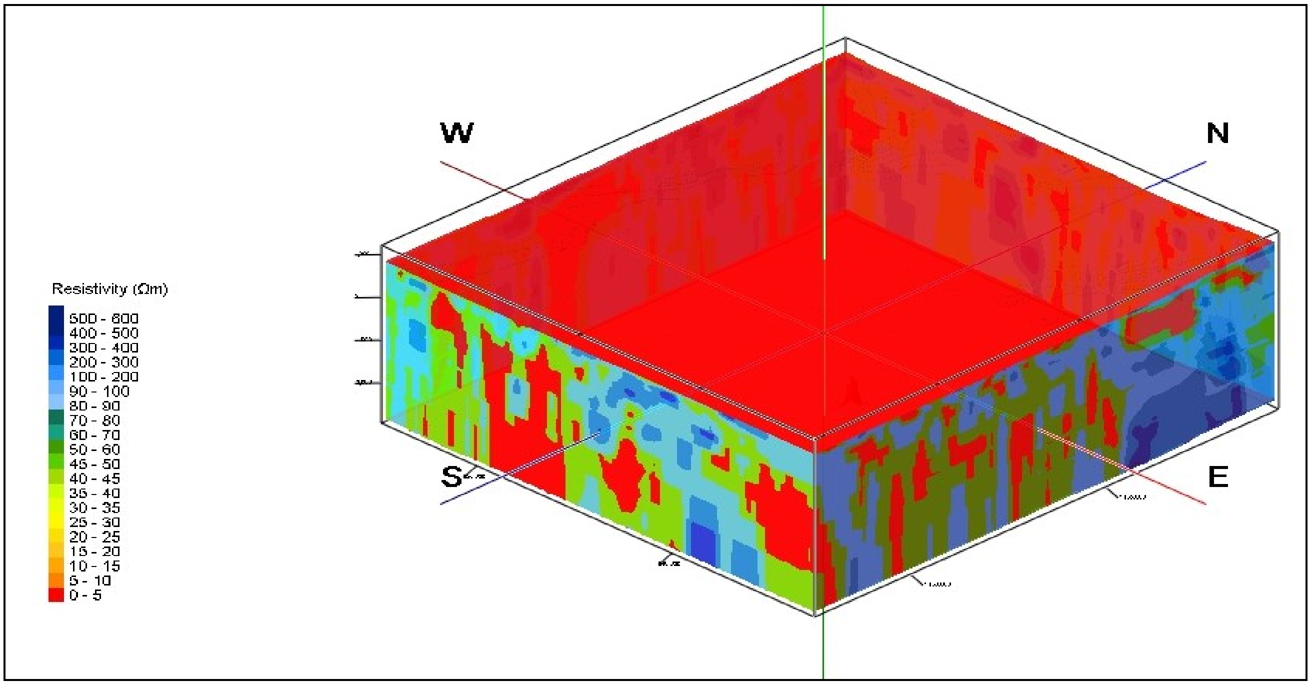

Figure 31: Isosurface resistivity model.

3.1.3 Lithology model

A solid lithology model for the Hágöngur area is given in Figure 4.

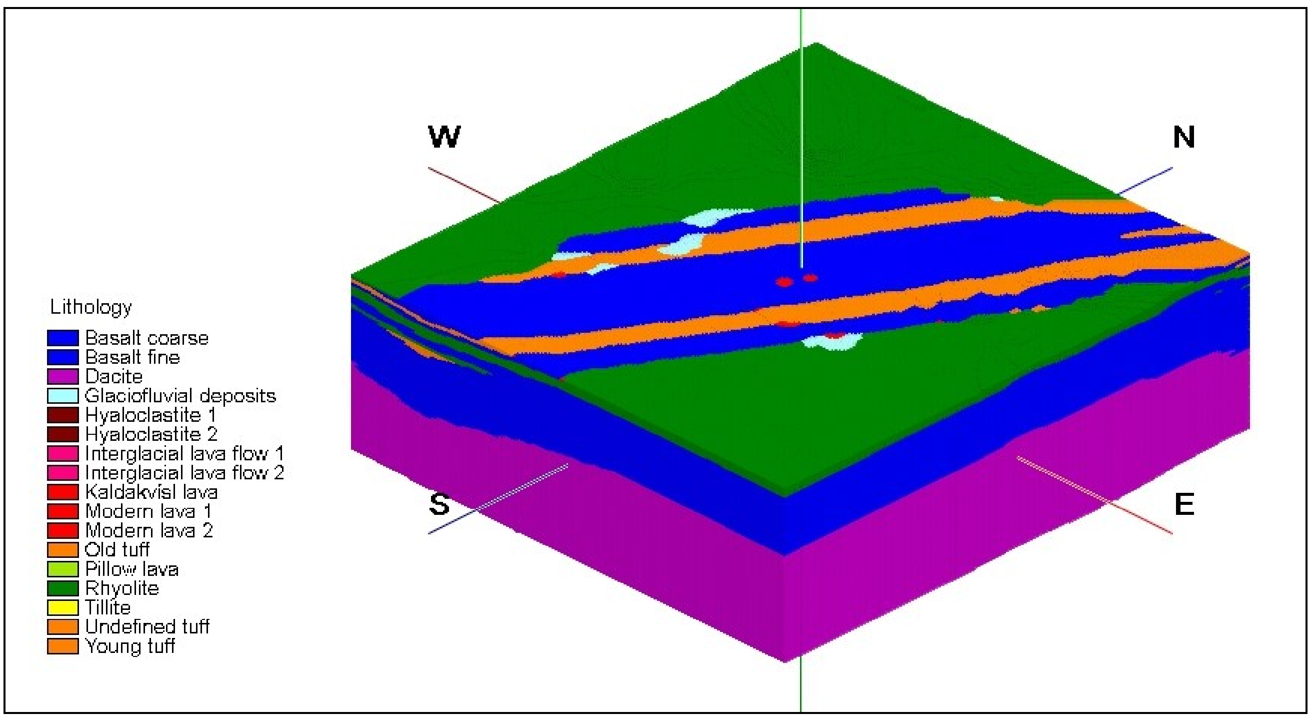

Figure 4: 3D lithology model of the Hágöngur area.

As shown in Figure 4, the upper layer of the Hágöngur reservoir is composed mainly by rhyolite, glaciofluvial deposits, modern lava and tuff ridges, followed by a thin basalt layer and then by a rhyolite layer that extends its edges to the highest elevation areas on top of the reservoir. Below these shallow layers, it is notable the presence of a thick basalt layer and finally a dacite layer in the bottom.

3.1.4 Stratigraphy models

The two stratigraphy solid models developed for the Hágöngur area are presented in Figure 5 and Figure 6.

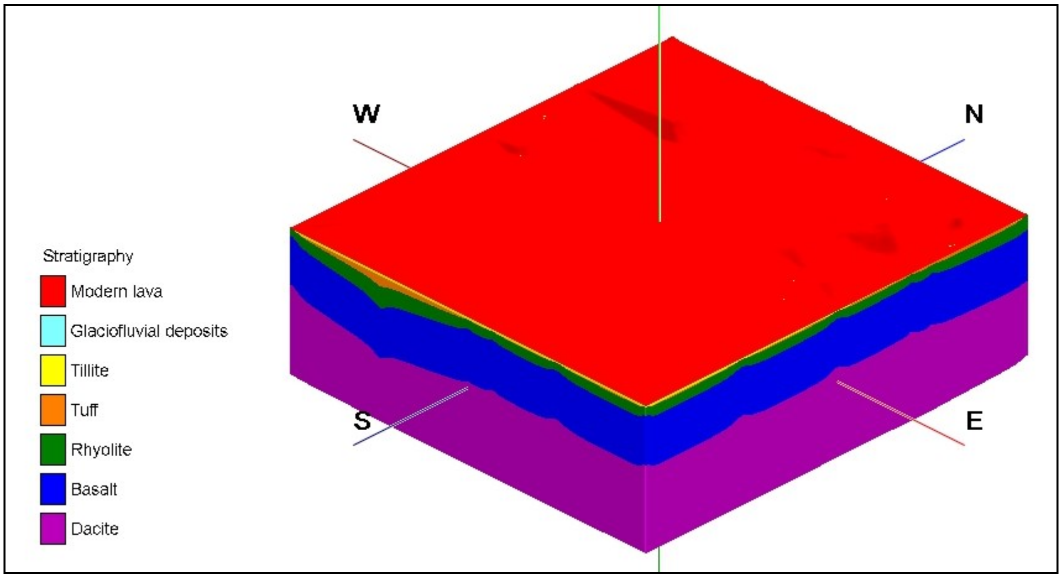

Figure 5: 3D stratigraphy solid Model 1.

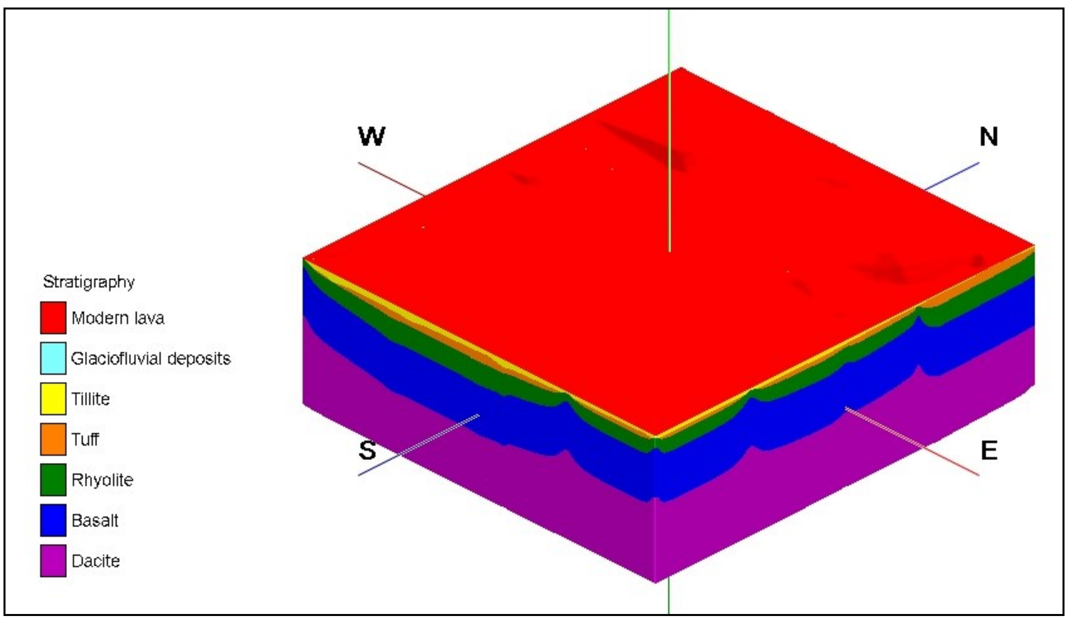

Figure 6: 3D stratigraphy solid Model 2.

The first stratigraphy model shown in Figure 5, follows the most probable pattern for the layers shape within the reservoir, where layers follow a gradual sinking of the stationary magma chamber in a V shape alignment. In contrast, the second stratigraphy model presented in Figure 6, shows planar shape layers in the middle of the magma chamber, with more pronounced slopes on the edges.

3.2 Conceptual modeling

Conceptual models per type of stratigraphy structure are shown in Figure 7 and Figure 8. In both cases, faults and their greater permeability allow the recharge of fluid in the reservoir. In contrast, the cap rock situated near the surface and its low permeability reduces the cold fluid infiltration from the top and the upwelling of hot fluid from the bottom.

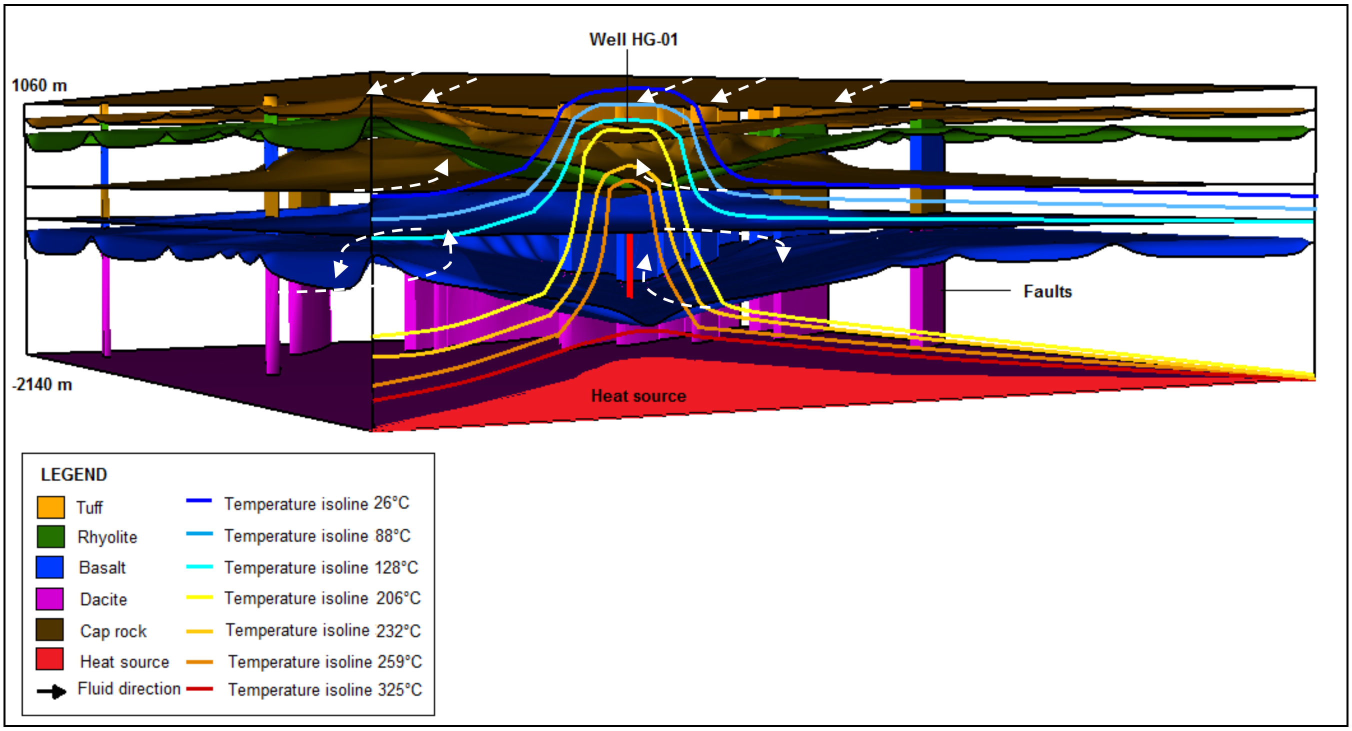

Figure 7: Conceptual model 1.

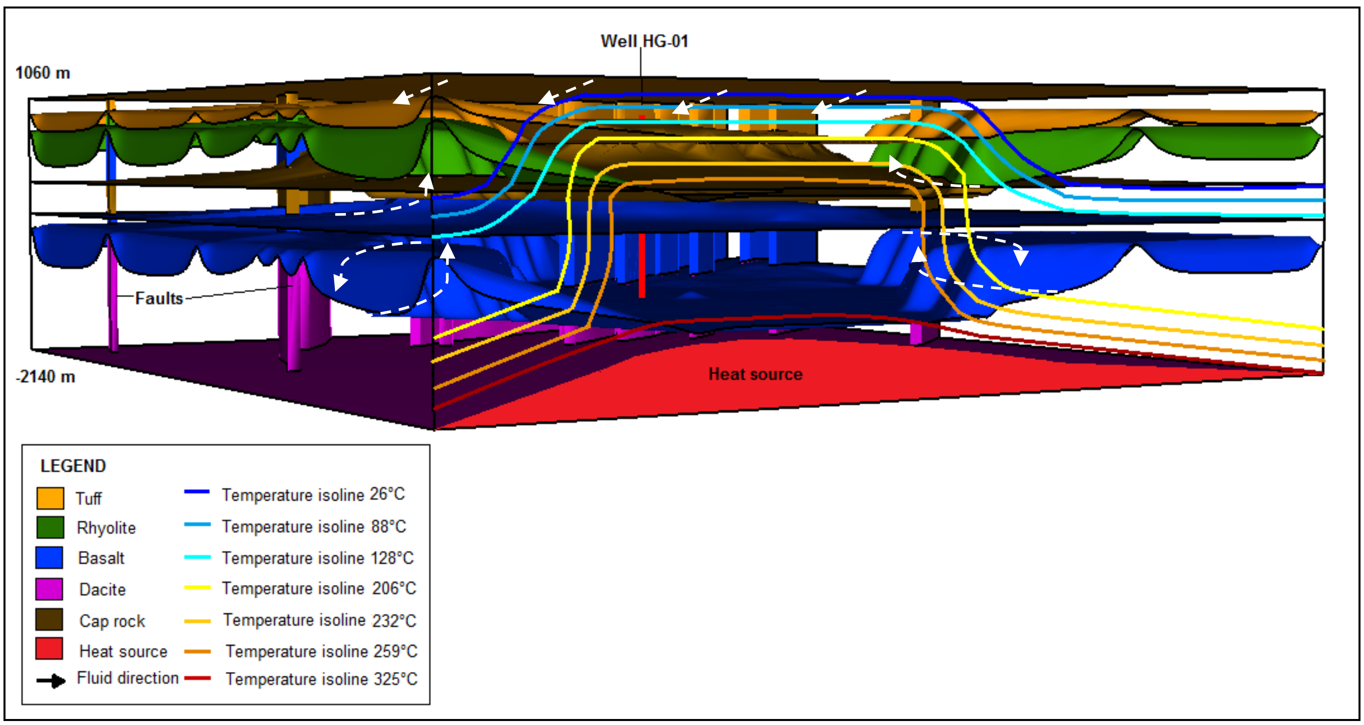

Figure 82: Conceptual model 2.

As illustrated in Figure 7 and Figure 8, a deep seated heat source allows the temperature increase in the middle of the reservoir and the upwelling of hot fluid with less density. As the fluid ascends, it gets mixed with colder denser fluid near the cap rock zone and descends again, forming convection cells between the heat source and the cap rock area.

The first model has higher pressure and temperature values within a thin zone in the middle of the reservoir, following the materials structure. In contrast, the second model has wide and planar temperature isosurfaces in the middle of the reservoir in accordance to the stratigraphy structure.

3.3 Numerical modeling

3.3.1 Natural state model for stratigraphy structure 1

The natural state model for the first stratigraphy structure was achieved after setting the following conditions:

- Initial temperature gradient of 100°C/km
- Hydrostatic pressure variation with depth among the layers
- Rock properties for the different layers presented in Table 1
- Permeability of 0.0001 mD in the cap rock area
- Permeability factor of 1000 among the faults cells
- Constant heat flux of 0.25 J/(s*m^2) in the bottom layer along with punctual heat sources with a constant flux of 1.0 J/(s*m^2) in the deepest middle part of the reservoir

The XY permeability distribution along the reservoir for the first stratigraphy structure is shown in Figure 9. The blue area represents the cap rock of the reservoir with very low permeability (0.0001 mD).

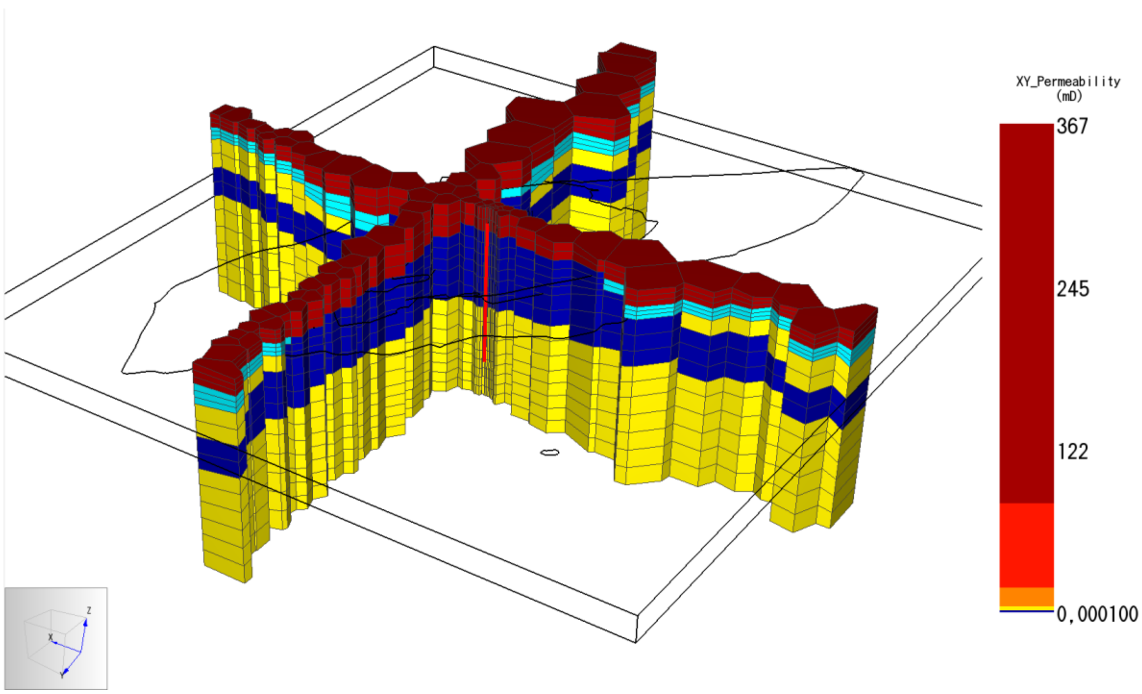

Figure 9: XY Permeability cross section for model 1

Additionally, it was necessary to make some changes in pressure values of the model boundaries, as well as changes in the Z direction permeability of dacite and the Z direction permeability of the last two bottom layers, which were decreased by a factor of 10^2 to avoid fluid infiltration.

The final temperature distribution reached in the natural state model for the first stratigraphy structure is shown in Figure 10, whereas pressure results are illustrated in Figure 11.

According to the natural state model temperature distribution shown in Figure 10, temperatures vary from 9.7 °C in the surface to 322°C in the heat source location. A relatively uniform pressure distribution with depth is observed in the natural state model as shown in Figure 11. Pressure values vary from 0.038 MPa in the surface up to 22.7 MPa in the bottom of the model (-2140 m depth).

On the other hand, it is observed fluid upflow from high to low temperature areas next to the heat source zone, which is conditioned by the presence of the cap rock; therefore, slightly convection is noticed in both sides of the heat source.

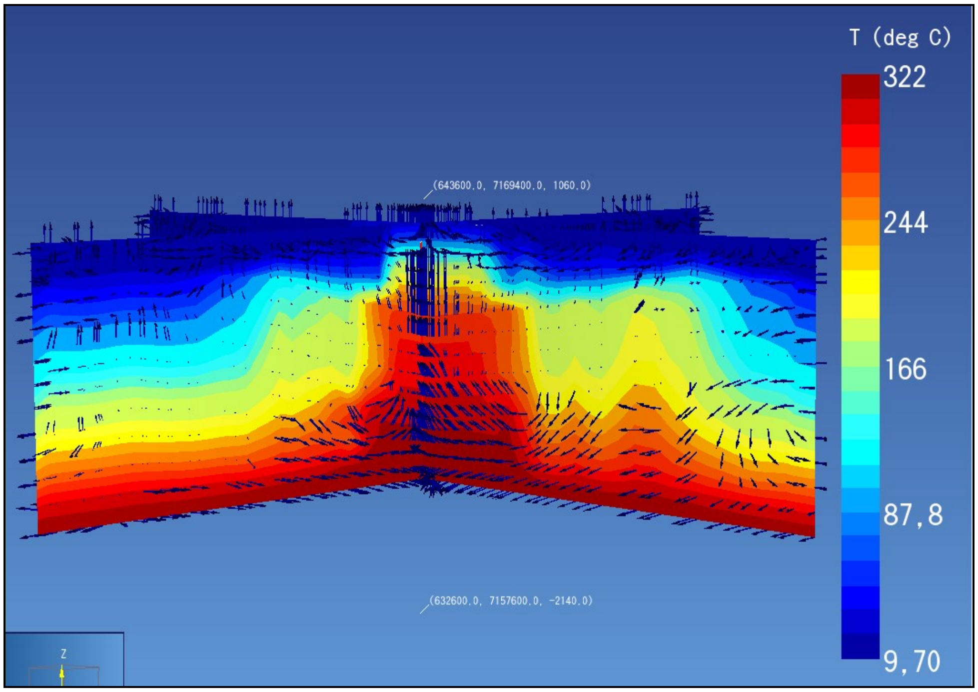

Figure 10: Natural state temperature distribution for model 1.

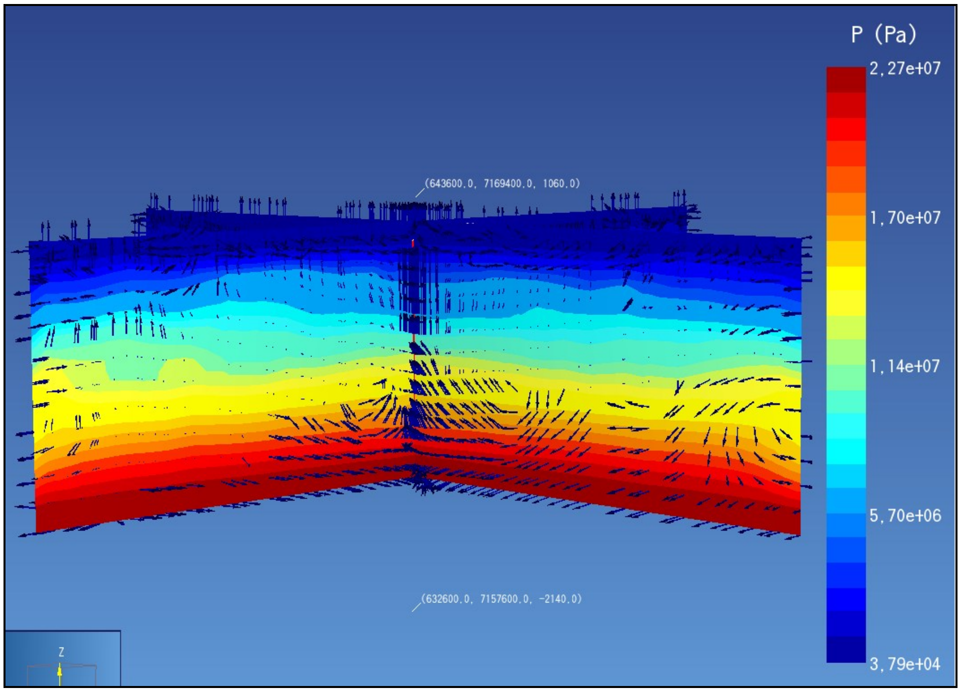

Figure 11: Natural state pressure distribution for model 1.

Finally, comparison graphs between observed and model simulated downhole pressure and temperature data are shown in Figure 12. Temperature values show a better match with depth than pressure values, which can be explained by the high grade of correlation between pressure and permeability. As the permeability in the Z direction of the bottom layer had to be decreased, pressure values on the layers above it increased due to more fluid upflow.

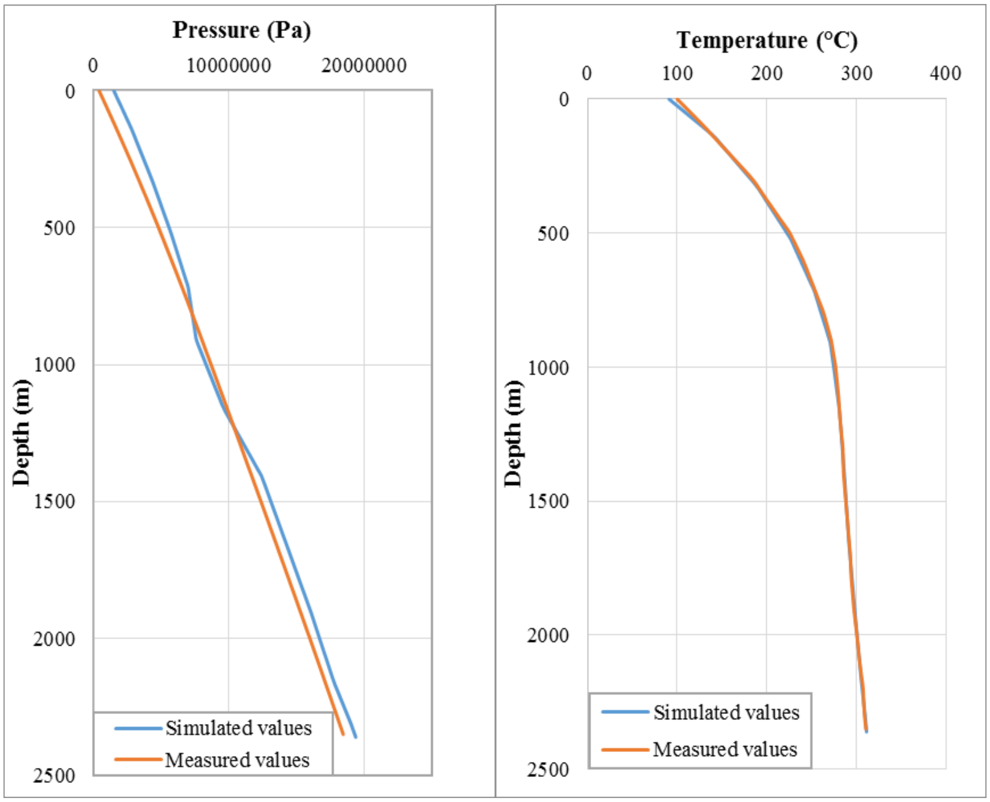

Figure 12: Comparison between observed and model simulated downhole pressure (left) and temperature (right) for the natural state model 1.

<u>3.3.2 Natural state model for stratigraphy structure 2</u>

The natural state model for the second stratigraphy structure was achieved after setting the same conditions as in the case of the first stratigraphy structure but changing the stratigraphy layers distribution. The permeability distribution and location of the cap rock for this model is shown in Figure 13.

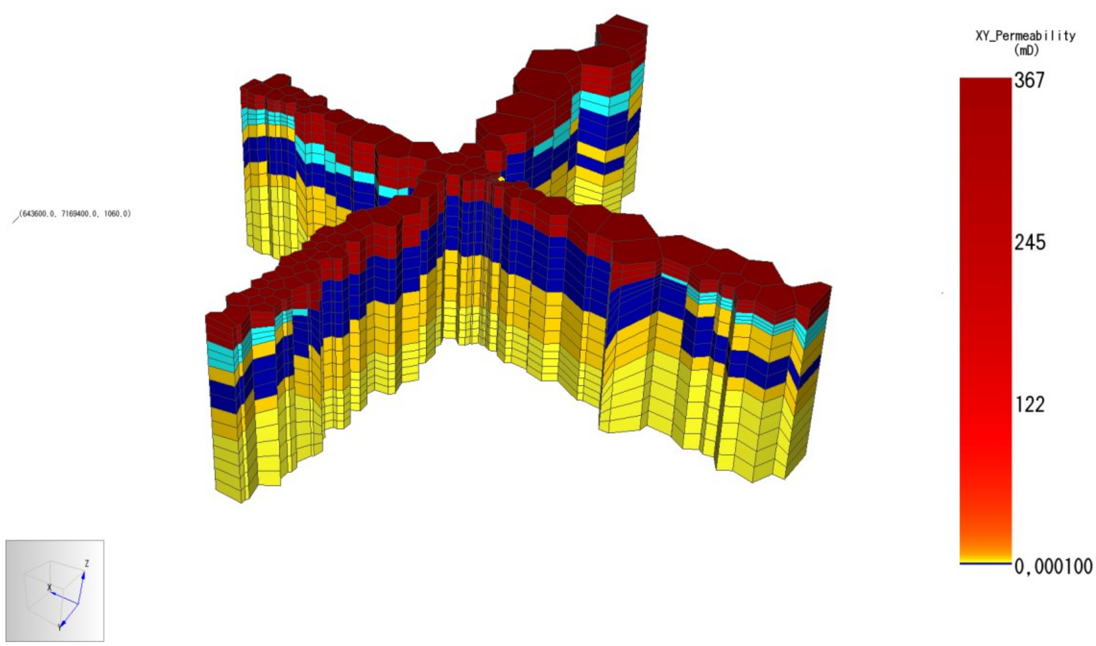

Figure 13: XY Permeability cross section for model 2

The final temperature profile under these conditions is shown in Figure 14, whereas pressure results are illustrated in Figure 15.

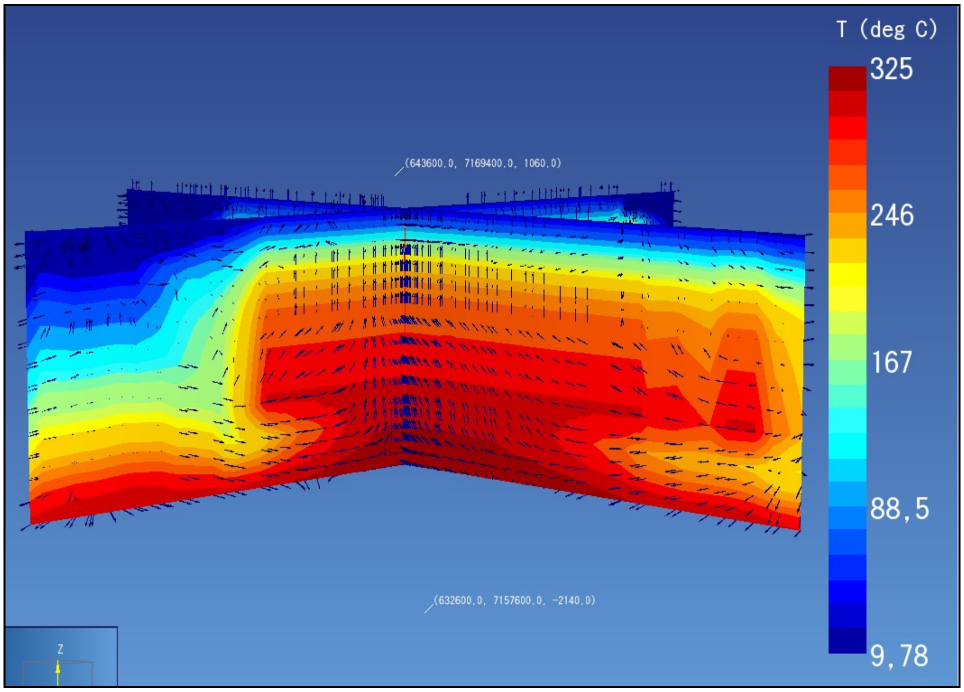

Figure 14: Natural state temperature distribution for model 2.

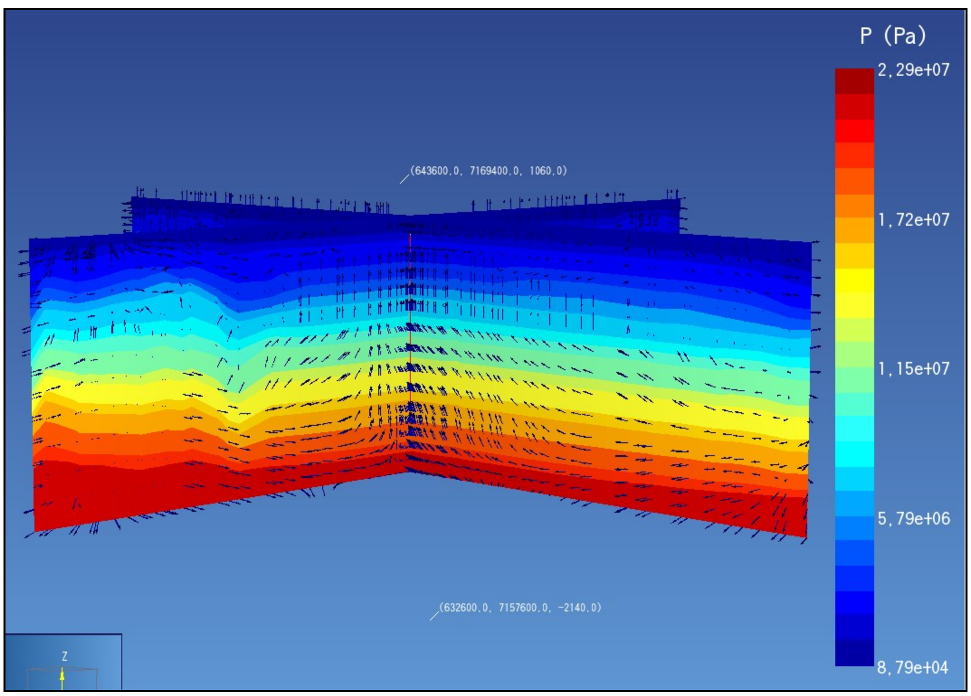

Figure 15: Natural state pressure distribution for model 2.

According to the natural state model, temperatures vary from 9.78 °C in the surface to 325°C in the heat source location, as shown in Figure 14.

A relatively uniform pressure distribution with depth is observed with the exception of higher pressures on the west side of the system, as shown in Figure 15. Pressure values vary from 0.0879 MPa in the surface up to 22.9 MPa in the bottom of the model (-2140 m depth).

On the other hand, it is observed fluid upflow from high to low temperature areas next and within the heat source zone, which is conditioned by the presence of the cap rock; therefore, slightly convection is noticed in both sides of the heat source.

Finally, comparison graphs between observed and simulated downhole pressure and temperature data are shown in Figure 16. Both, temperature and pressure values show a better match from 1000 meters depth in the well, which represents an elevation of 181 m.b.s.l.

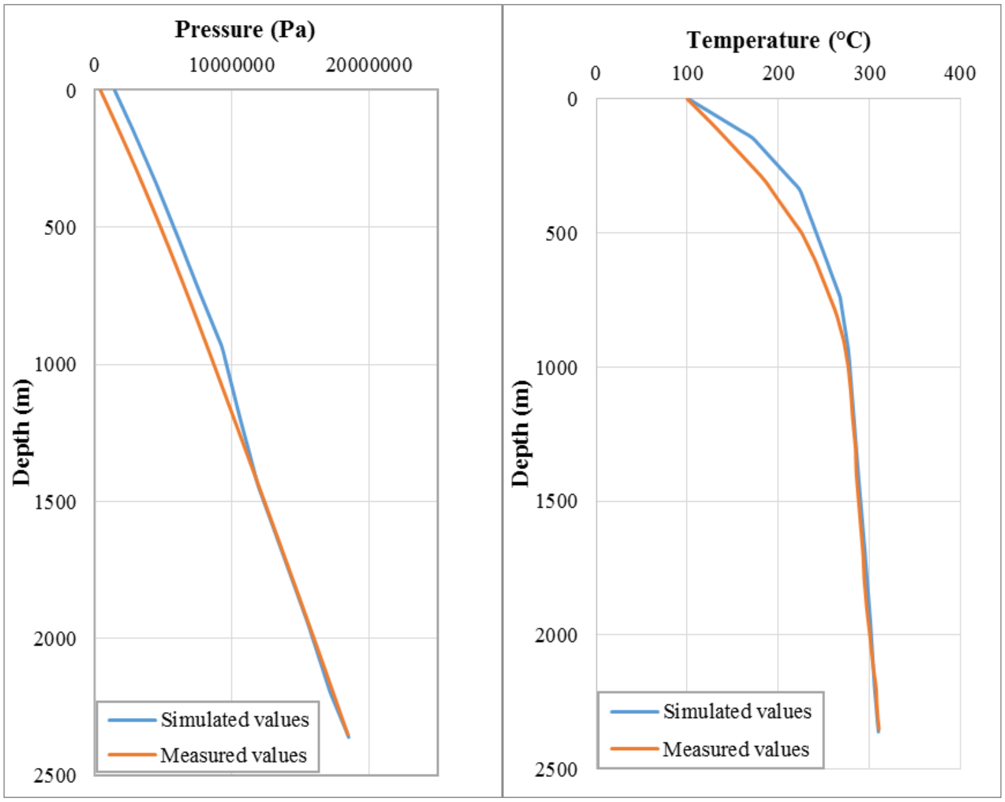

Figure 16: Comparison between observed and model simulated downhole pressure (left) and temperature (right) for the natural state model 2.

4. CONCLUSIONS

Two versions of conceptual and natural state models were developed for the Hágöngur geothermal system over the basis of two different stratigraphy structures. These models cover a superficial area of 129.8 km^2 and a total thickness of 3.2 km, and they have the deep well HG-01 in the middle of the boundary in accordance with previous resistivity surveys.

The natural state model for the first stratigraphy structure has a better correlation of pressure and temperature values with available downhole data of Well HG-01 than the model for the second stratigraphy structure.

Parameters that affect the models the most are: Permeability in the Z direction, which represents an increase in pressure due to the increase in fluid inflow into the system; placement of the cap rock, that leads an increase in pressure on top of it and a disturbance in temperature values; and finally the initial pressure conditions set for the boundaries of the system, which conditions the direction of the fluid inflow into the system and the formation of convection cells on both sides of the high temperature area of the system.

Further improvements to the current assessment can be made through the generation of additional models with smaller and larger heat sources areas for both types of stratigraphy structures, in order to compare the reservoir's behavior under these different conditions.

On the other hand, it is recommended updating both, conceptual and natural state models when more downhole information is available. Finally, it is recommended the usage of these numerical models to assess the uncertainty in the production capacity of the reservoir, and the location of potential drilling targets.

REFERENCES

Ágústsdóttir, Þ. (2009). On the Dynamics of Rhyolite Dome Emplacement: Densities and Deformation Fields. University of Iceland. Reykjavik, Iceland.

Eppelbaum, L., Kutasov, I., & Pilchin, A. (2014). Applied Geothermics. Springer. Berlin, Germany.

Heiken, G. (2006). Tuffs. Their properties, Uses, Hydrology, and Resources. The Geological Society of America. Colorado, United States of America.

Hjartarson, Á. (2015). Heat Flow in Iceland. Proceedings World Geothermal Congress 2015. Melbourne, Australia.

Jonsson, S. S., Gudmundsson, A., & Palsson, B. (2005). The Hágöngur High-Temperature Geothermal Field, Central-Iceland. Surface Exploration and Drilling of the First Borehole: Lithology, Alteration and Geological Setting. Proceedings World Geothermal Congress 2005 (pp. 1-6). Antalya, Turkey.

Karlsdóttir, R., & Vilhjálmsson, A. M. (2013). Hágöngur Geothermal Area, Iceland. 3D Inversion of MT Data. Landsvirkjun. Reykjavik, Iceland.

Karlsdóttir, R., Vilhjálmsson, A. M., Eysteinsson, H., & Árnason, K. (2007). Köldukvíslarbotnar. TEM-mælingar 2007. ÍSOR (Iceland Geosurvey). Reykjavik, Iceland.

Stefánsson, V., Sigurðsson, Ó., Guðmundsson, Á., Franzson, H., Friðleifsson, G. Ó., & Tulinius, H. (1997). Core Measurements and Geothermal Modelling. Second Nordic Symposium on Petrophysics (bls. 199-220). Nordic Petroleum Technology Series One. Reykjavik, Iceland.

Wohletz, K., & Heiken, G. (1992). Volcanology and Geothermal Energy. University of California Press. Berkeley, Los Angeles, Oxford.

Zou, C. (2013). Volcanic Reservoirs in Petroleum Exploration. Elsevier. China.